

## Original Research Article

# Culture-free identification of fast-growing cyanobacteria cells by Raman-activated gravity-driven encapsulation and sequencing

Jinyu Cui<sup>a,b,c,1</sup>, Rongze Chen<sup>a,b,c,d,1</sup>, Huili Sun<sup>a,b,c,d,1</sup>, Yingyi Xue<sup>a,b,c</sup>, Zhidian Diao<sup>a,b,c,d</sup>,  
Jingyun Song<sup>a,b,c</sup>, Xiaohang Wang<sup>a,b,c</sup>, Jia Zhang<sup>a,b,c</sup>, Chen Wang<sup>a,b,c</sup>, Bo Ma<sup>a,b,c</sup>,  
Jian Xu<sup>a,b,c,d,f,\*\*</sup>, Guodong Luan<sup>a,b,c,d,e,\*\*\*</sup>, Xuefeng Lu<sup>a,b,c,d,e,f,\*</sup>

<sup>a</sup> Key Laboratory of Biofuels, Qingdao Institute of Bioenergy and Bioprocess Technology, Chinese Academy of Sciences, No. 189 Songling Road, Qingdao, 266101, China

<sup>b</sup> Shandong Energy Institute, Qingdao, 266101, China

<sup>c</sup> Qingdao New Energy Shandong Laboratory, Qingdao, 266101, China

<sup>d</sup> College of Life Science, University of Chinese Academy of Sciences, Beijing, China

<sup>e</sup> Dalian National Laboratory for Clean Energy, Dalian, 116023, China

<sup>f</sup> Laboratory for Marine Biology and Biotechnology, Qingdao National Laboratory for Marine Science and Technology, Qingdao, China



## ARTICLE INFO

## Keywords:

Cyanobacteria  
Single-cell Raman microspectroscopy  
Stable isotope probing  
Carotenoids  
Identification

## ABSTRACT

By directly converting solar energy and carbon dioxide into biobased products, cyanobacteria are promising chassis for photosynthetic biosynthesis. To make cyanobacterial photosynthetic biosynthesis technology economically feasible on industrial scales, exploring and engineering cyanobacterial chassis and cell factories with fast growth rates and carbon fixation activities facing environmental stresses are of great significance. To simplify and accelerate the screening for fast-growing cyanobacteria strains, a method called Individual Cyanobacteria Vitality Tests and Screening (iCyanVS) was established. We show that the <sup>13</sup>C incorporation ratio of carotenoids can be used to measure differences in cell growth and carbon fixation rates in individual cyanobacterial cells of distinct genotypes that differ in growth rates in bulk cultivations, thus greatly accelerating the process screening for fastest-growing cells. The feasibility of this approach is further demonstrated by phenotypically and then genotypically identifying individual cyanobacterial cells with higher salt tolerance from an artificial mutant library via Raman-activated gravity-driven encapsulation and sequencing. Therefore, this method should find broad applications in growth rate or carbon intake rate based screening of cyanobacteria and other photosynthetic cell factories.

## 1. Introduction

Cyanobacteria are the only group of prokaryotes that perform oxygen-generating photosynthesis, thus they serve as an important source of primary productivity in the biosphere [1]. In recent years, cyanobacteria are considered promising chassis for photosynthetic biosynthesis, due to their capability of directly converting solar energy

and carbon dioxide into various biobased products [2,3]. Compared with higher plants and eukaryote algae, cyanobacteria possess shorter life cycles, faster growth, simpler structures, and more efficient photosynthesis, thus are attractive microbial photosynthetic platforms for biotechnological and industrial applications [4]. For example, cyanobacterial strains have been cultivated to produce high-value secondary metabolites, such as carotenoid, mycosporine-like amino acids, and

Peer review under responsibility of KeAi Communications Co., Ltd.

\* Corresponding author. Key Laboratory of Biofuels, Qingdao Institute of Bioenergy and Bioprocess Technology, Chinese Academy of Sciences, No. 189 Songling Road, Qingdao, 266101, China.

\*\* Corresponding author. Key Laboratory of Biofuels, Qingdao Institute of Bioenergy and Bioprocess Technology, Chinese Academy of Sciences, No. 189 Songling Road, Qingdao, 266101, China.

\*\*\* Corresponding author. Key Laboratory of Biofuels, Qingdao Institute of Bioenergy and Bioprocess Technology, Chinese Academy of Sciences, No. 189 Songling Road, Qingdao, 266101, China.

E-mail addresses: [xujian@qibebt.ac.cn](mailto:xujian@qibebt.ac.cn) (J. Xu), [luangd@qibebt.ac.cn](mailto:luangd@qibebt.ac.cn) (G. Luan), [lvxf@qibebt.ac.cn](mailto:lvxf@qibebt.ac.cn) (X. Lu).

<sup>1</sup> These three authors contributed equally to the paper.

<https://doi.org/10.1016/j.synbio.2023.11.001>

Received 31 August 2023; Received in revised form 3 November 2023; Accepted 5 November 2023

Available online 11 November 2023

2405-805X/© 2023 The Authors. Publishing services by Elsevier B.V. on behalf of KeAi Communications Co. Ltd. This is an open access article under the CC BY-NC-ND license (<http://creativecommons.org/licenses/by-nc-nd/4.0/>).

scytonemin [5,6]. Moreover, synthetic biology approaches have been adopted to improve the photosynthesis productivity of cyanobacteria chassis cells and cell factories and to remodel the photosynthetic metabolism network for the photosynthetic production of multiple natural or nonnatural metabolites [7]. However, industrial application of cyanobacterial photosynthetic biosynthesis is still hindered by multiple factors, e.g., the weak cellular robustness of cyanobacterial chassis cells and cell factories when facing environmental stresses in industrial systems and processes [8]. Cyanobacterial strains of rapid growth and efficient carbon fixation are the foundation for large-scale cultivation in actual industrial environments. Therefore, rapid and reliable methods to identify strains with such phenotypes from the natural environment or from mutant libraries are of keen interest [9].

The traditional paradigm for phenotypic screening of cyanobacteria is based on culture, e.g., plate-based colony cultivation followed by liquid culture. Due to the lower growth rate of such photoautotrophic cells than heterotrophic cells such as *Escherichia coli* or yeast, this paradigm is very time-consuming and of low throughput, especially when cultivated under stress conditions. Single-cell-based selection methods provide a solution to tackle these challenges [10–12]. Single-cell is the basic unit of life forms and the atomic step of biological evolution on Earth, thus single-cell technologies for phenotypic or genotypic analysis at single-cell resolution can dissect and mine biological devices, modules or chassis with unprecedented precision [13, 14]. On the other hand, for the purpose of phenotype screening, single-cell technologies can greatly shorten or even completely skip the tedious and time-consuming cultivation and propagation of cells [15]. Therefore, single-cell technologies have supported phenotype-based profiling and screening of cyanobacteria [16], particularly for product-related phenotypes (i.e., yield of target chemicals [17–20]). For instance, as cyanobacteria contain chlorophyll which exhibits some level of fluorescence and can serve a measure of the number of cells, a microdroplet platform was introduced for screening fast-growing cyanobacteria from two cyanobacterial species which monitors intracellular natural chlorophyll autofluorescence after 4 days of in-droplet growth, however it is unable to sort cyanobacteria due to their small cell size [9]. Meanwhile, a droplet-based microfluidic workflow was proposed that combines several microfluidic devices to encapsulate, assay, and sort L-lactate-producing strains of the cyanobacterium *Synechocystis* sp. PCC 6803 (hereafter PCC 6803) based on fluorescence monitoring after addition of lactate assay enzyme solution [18]. These approaches are all intrinsically growth-based, thus remain slow and inefficient.

Here we ask whether it is possible to screen cyanobacteria for growth rate at single-cell resolution, i.e., to predict the growth rate of cyanobacteria without actually tracking its cellular multiplication. A single-cell Raman spectrum (SCRS) can serve as an intrinsic biochemical fingerprint of individual cells that is label-free and non-invasive features [21–23]. Moreover, SCRS can be exploited to track substrate intake, as the incorporation of stable isotopes in substrate into intracellular macromolecules would lead to the “red-shift” of corresponding Raman bands in SCRS [24,25]. Such Stable Isotope Probing based Raman Microspectroscopy (Raman-SIP) was employed to probe substrate-specific metabolism at the single-cell resolution [20,26–28]. For example, to tackle the challenges associated with methods that are based on cellular growth, deuterium-probing based SCRS was proposed for quantitative assessment of vitality [29] and antimicrobial susceptibility [20,25,30]. However, although cellular growth is clearly dependent on substrate consumption by the cell, it is not clear whether, to what degree, or under what circumstances the substrate intake rate revealed at SCRS at the single-cell resolution is correlated with the growth rate of the strain.

In this study, we introduce a culture-free, one-cell-resolution, phenome-genome-combined strategy called Individual Cyanobacteria Vitality Tests and Screening (iCyanVS). We show that the  $^{13}\text{C}$  incorporation ratio of carotenoids in individual, genetically heterogeneous cyanobacterial cells can be used to measure differences of their growth rate and carbon fixation rate in bulk cultivations. The potential and

**Table 1**

The cyanobacterial mutant strains and plasmids used in this study.

Strains/Plasmids	Genotype or relevant features	References
Plasmids		
pSI	NSI::P <sub>cpcB1</sub> -mcs-TrbcL; Km <sup>R</sup>	[31]
pJC56	NSI::P <sub>cpcB1</sub> -rpoD1-TrbcL	This study
pJC57	NSI::P <sub>cpcB1</sub> -rpoD2-TrbcL	This study
pJC59	NSI::P <sub>cpcB1</sub> -rpoD4-TrbcL	This study
pJC62	NSI::P <sub>cpcB1</sub> -sigG-TrbcL	This study
pJC63	NSI::P <sub>cpcB1</sub> -sigI-TrbcL	This study
pJC64	NSI::P <sub>cpcB1</sub> -sigF-TrbcL	This study
Strains		
PCC 7942	PCC 7942 wild-type (WT)	
JC19	NSI::P <sub>cpcB1</sub> -rpoD1-TrbcL	This study
JC20	NSI::P <sub>cpcB1</sub> -rpoD2-TrbcL	This study
JC22	NSI::P <sub>cpcB1</sub> -rpoD4-TrbcL	This study
JC25	NSI::P <sub>cpcB1</sub> -sigG-TrbcL	This study
JC26	NSI::P <sub>cpcB1</sub> -sigI-TrbcL	This study
JC27	NSI::P <sub>cpcB1</sub> -sigF-TrbcL	This study

robustness of this approach were further demonstrated by identifying cells with higher salt tolerance from an artificial mutant library by Raman-activated gravity-driven encapsulation and sequencing. The iCyanVS strategy has the advantages of being culture-free, identifying single-cell metabolic activity from single-cell accuracy, high throughput, and high accuracy.

## 2. Materials and methods

### 2.1. Bacterial growth conditions

The *Synechococcus elongatus* PCC 7942 (hereafter PCC 7942) and engineered strains were grown on BG11 agar plates or in BG11 medium (pH 7.5) under a light intensity of  $\sim 150 \mu\text{mol photons m}^{-2}\text{s}^{-1}$  in an illuminating or shaking incubator at 130 rpm and 30 °C (HNYC202T, Honor, Tianjin, China) [31]. The appropriate antibiotic, e.g., 20  $\mu\text{g/mL}$  kanamycin (Solarbio, Beijing, China), was added to maintain the stability of the engineered strains. Optical density of culture was measured by a spectrophotometer (UV1750, Shimadzu, Kyoto, Japan) at 750 nm. *Escherichia coli* DH5 $\alpha$  was grown on LB agar plates or in LB liquid medium in an incubator at 37 °C or shaking incubator at 200 rpm supplemented with 50  $\mu\text{g/mL}$  kanamycin or 200  $\mu\text{g/mL}$  ampicillin (Solarbio, Beijing, China).

For  $^{13}\text{C}$  labeling culture, PCC 7942 was cultured for logarithmic time and then transferred to culture medium with 100 mM  $\text{NaH}^{13}\text{CO}_3$  as the only carbon source for labeled culture. Samples were taken at different time points for Ramanome acquisition and data analysis [32]. For high-light-stress culture, all the strains were precultured for 24 h under a light intensity of  $\sim 500 \mu\text{mol photons m}^{-2}\text{s}^{-1}$  and then transferred to culture medium with  $\text{NaH}^{13}\text{CO}_3$  as the only carbon source for 12 h of culture under a light intensity of  $\sim 1400 \mu\text{mol photons m}^{-2}\text{s}^{-1}$ . For salt-stress culture, all the strains were precultured for 24 h under 0.3 M NaCl conditions and then transferred to culture medium with  $\text{NaH}^{13}\text{CO}_3$  as the only carbon source for 12 h and under 0.35 M NaCl.

### 2.2. Construction of plasmids and strains

The strains and plasmids used in this study are listed in Table 1. Among them, *E. coli* DH5 $\alpha$  was used for vector construction and amplification. For gene overexpression, the integrative vector pSI with a kanamycin-resistant cassette was used [31]. Primers for gene amplification are listed in Supplementary Table 1. All primers were synthesized by GENEWIZ Inc. (Suzhou, China). The target genes were amplified by Phanta Super-Fidelity DNA Polymerase (Vazyme Biotech, Nanjing, China) and purified by a Cycle Pure Kit (Omega Bio-Tek, Norcross, GA, United States), and then the gene products were ligated into pSI (linearized by PCR) by using the ClonExpress® Ultra One Step Cloning Kit

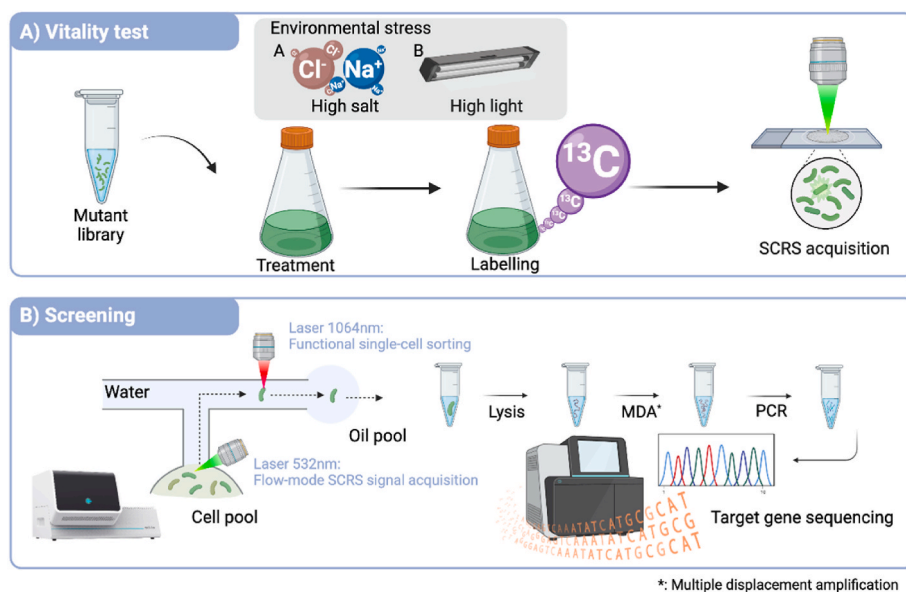


**Fig. 1.** Overview of the iCyanVS strategy. A) Experimental procedure of the vitality test. For example, the mutant library was pretreated under environmental stresses (e.g., high light and high salt) and then incubated with  $\text{NaH}^{13}\text{CO}_3$ . After a certain period, the sample would undergo SCRS acquisition. B) The RAGE-Seq workflow for one-cell-resolution phenotype screening and genotype sequencing. After stress exposure and then the  $\text{NaH}^{13}\text{CO}_3$  feeding, cells that exhibit higher vitality would carry a strong  $^{13}\text{C}$  incorporation ratio, suggesting stronger stress tolerance and correspondingly, higher growth rate under stress. These mutant cells were then sorted, lysed, amplified and sequenced by the RAGE-Seq technique in a RACS-Seq instrument (Methods).

(Vazyme Biotech, Nanjing, China). All constructs were validated by colony PCR and confirmed by Sanger sequencing. The constructed plasmid was transformed into PCC 7942 according to a method reported previously [33]. Briefly, 2 mL of WT with an  $\text{OD}_{730\text{nm}}$  of 1.0 was centrifuged at  $6000\times g$  for 5 min and then resuspended in 250  $\mu\text{L}$  of fresh BG11 medium. Next, 200 ng plasmid was added and incubated in the dark at 150 rpm and  $30^\circ\text{C}$  for 6–24 h. Then, the mixtures were plated on solid BG11 plates with 1.5 % agar after transformation and incubated at  $30^\circ\text{C}$  and 150  $\mu\text{mol photons m}^{-2}\text{s}^{-1}$  for 5 days. The obtained colonies were picked, streaked on fresh BG11 plates, and incubated for another 5 days under the same conditions. Genotypes of the transformants were examined by amplifying the targeted genes for Sanger sequencing.

### 2.3. Acquisition of single-cell Raman spectra

The sample was prepared as previously described [34,35]. Briefly, cells were collected by centrifuging at  $8000\times g$  for 1 min and then washed three times using Milli-Q water. An aliquot of the sample (1.5  $\mu\text{L}$ ) was spotted on  $\text{CaF}_2$  slides with a low background signal and dehydrated in air at room temperature. Raman spectra were acquired in the range of  $400\text{--}2000\text{ cm}^{-1}$  with a spectral resolution of  $\sim 2\text{ cm}^{-1}$  and using a confocal micro-Raman system armed by an excitation laser (532 nm Nd: YAG) and a diffraction grating (900 grooves/mm). A dry objective (100 $\times$ ) with a numerical aperture of 0.9 (Olympus, Japan) was used for the observation of cyanobacteria cells and Raman signal acquisition. The laser power on the sample plane was  $\sim 0.1\text{ mW}/\mu\text{m}^2$ . The acquisition time for the individual spectrum was 0.1 s, and at least 100 valid single-cell spectra were attained from each sample following quality control.

### 2.4. Raman-activated cell sorting and sequencing (RACS-Seq)

Before conducting the RACS-Seq experiment, all reagents and consumable materials were ultraviolet irradiated for 10 min in a Spectrolinker XL-1500 to remove pollution. Then, the commercial mutant library sample was dissolved in Milli-Q water and shaken for 5–10 min to dissolve completely. After centrifugation at  $8000\times g$  for 1 min, the supernatant was removed and the cells in suspension were washed three

times with  $\text{ddH}_2\text{O}$  and diluted to a proper density ( $\approx 10^6\text{ CFU/mL}$ ). Then, the cellular sample was injected into a RACS-Seq chip on the height-adjustable sample holder for SCRS acquisition and sorting. After loading the chip onto the RACS-Seq instrument (Qingdao Single-cell Biotech, China), a 10x dry objective was used for observation of droplet generation and transportation, while a 60x water objective was used for both SCRS acquisition and optical tweezer. The cells in the detection fields were captured with optical tweezer (the 1064 nm laser at 300 mW), and with SCRS acquisition (the 532 nm laser at 0.1 mW for 1 s; the  $^{13}\text{C}$  ratios used for quantifying cells viability). Thus, SCRS-based phenotypes and subsequent genotypes were linked in an accurately indexed manner at single-cell resolution.

### 2.5. Multiple displacement amplification (MDA) and functional gene sequencing of sorted cyanobacteria cells

Before performing the MDA experiment which is a prerequisite for sequencing the cells sorted by the RACS-Seq instrument, all reagents and consumable materials were ultraviolet irradiated for 10 min in a Spectrolinker XL-1500. Then each sorted single cell (one cell per PCR tube) was lysed with 1  $\mu\text{L}$  lysis buffer with a transient vortex at  $65^\circ\text{C}$  for 10 min, followed by the addition of 1  $\mu\text{L}$  of stop solution (B buffer) to neutralize the lysis buffer. After gentle shaking, 30  $\mu\text{L}$  of reagents containing 6 N primers, dNTPs, DTT, and phi29 DNA polymerase were added and incubated at  $30^\circ\text{C}$  for 8 h (T100, Bio-Rad, USA). Negative control reactions without cells or DNA templates were carried out in parallel, to detect and quantify potential contamination from the laboratory environment. All reagents were from the Single-cell Whole-genome Amplification Kit (Qingdao Single-Cell Biotech, Qingdao, China).

For sequencing the NSI gene in the sorted individual cyanobacteria cells, we designed a two-round specificity PCR. The first-round PCR mixture contained 10  $\mu\text{L}$  of  $2\times\text{Taq Mix}$  (Monad Biotech Co., Ltd., Wuhan, China), 1  $\mu\text{L}$  NSI-F1 primer (10  $\mu\text{M}$ ), 1  $\mu\text{L}$  NSI-R1 primer (10  $\mu\text{M}$ ), 7  $\mu\text{L}$  nuclease-free water and 1  $\mu\text{L}$  MDA products. The 16S PCR program was as follows:  $94^\circ\text{C}$  for 5 min, 30 cycles of  $94^\circ\text{C}$  for 30 s,  $56^\circ\text{C}$  for 90 s,  $72^\circ\text{C}$  for 1.5 min and  $72^\circ\text{C}$  for 10 min. The second-round PCR mixture contained 10  $\mu\text{L}$  of  $2\times\text{Taq Mix}$  (Monad Biotech Co., Ltd., Wuhan,

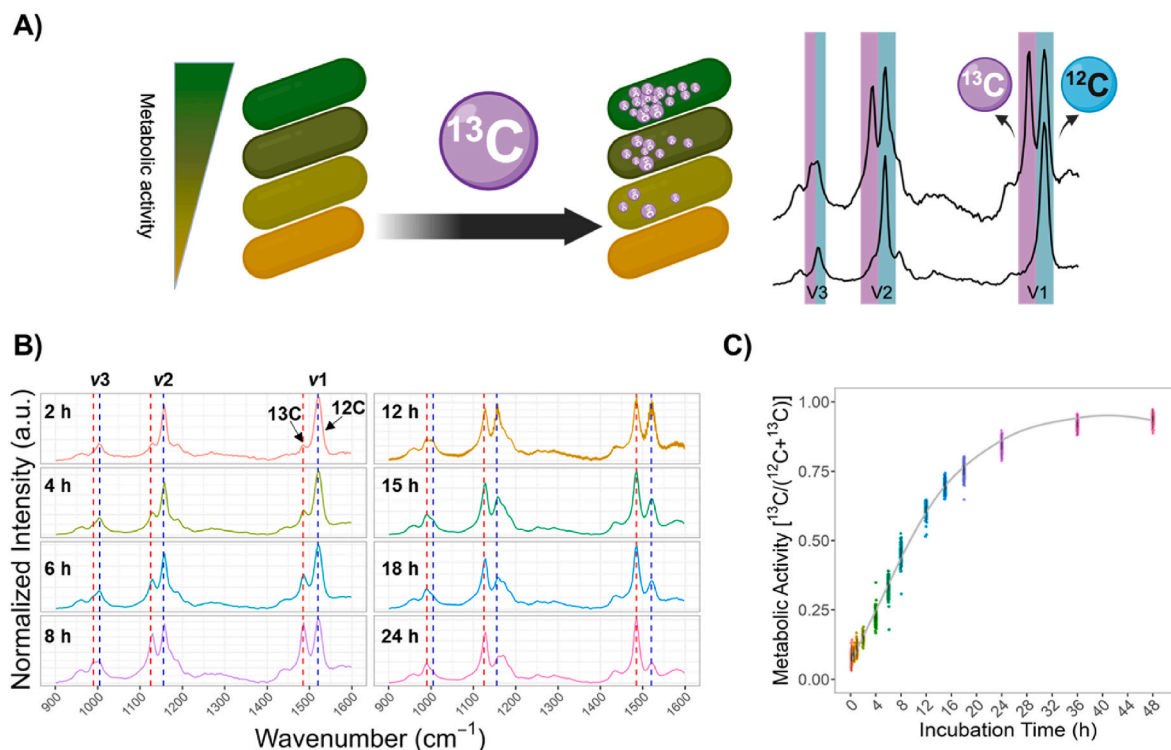


**Fig. 2.** Measurement of cyanobacterial single-cell metabolic vitality based on Raman-SIP. A) Schematic diagram of stable isotope labeling of individual cyanobacterial cells for vitality measurement. Cells that exhibit different vitality would carry distinct  $^{13}\text{C}$  incorporation ratios. Cells with higher vitality would show stronger  $^{13}\text{C}$  incorporation ratio (the upper Raman spectrum), and cells with lower vitality exhibit lower  $^{13}\text{C}$  incorporation ratio (the bottom spectrum). B) The Raman spectra of cells incubated with  $\text{NaH}^{13}\text{CO}_3$  for different times, normalized by the sum of the fingerprint area from 900 to 1600  $\text{cm}^{-1}$ . The Raman bands of  $\nu_1$ ,  $\nu_2$ , and  $\nu_3$  displayed a red-shift due to  $^{13}\text{C}$  incorporation in cells; C)  $^{13}\text{C}$  incorporation dynamics observed at the single-cell level. The  $^{13}\text{C}$  incorporation ratio at a certain time was used to represent metabolic activity.

China), 1  $\mu\text{L}$  NSI-F2 primer (10  $\mu\text{M}$ ), 1  $\mu\text{L}$  NSI-R2 primer (10  $\mu\text{M}$ ), 7  $\mu\text{L}$  nuclease-free water and 1  $\mu\text{L}$  MDA products. The second-round PCR program was as follows: 94  $^\circ\text{C}$  for 5 min, 30 cycles of 94  $^\circ\text{C}$  for 30 s, 55  $^\circ\text{C}$  for 30 s, 72  $^\circ\text{C}$  for 1 min, and 72  $^\circ\text{C}$  for 10 min.

## 2.6. Data analysis of single-cell Raman spectra

The principle of quality control is removing those spectra that represent background signal, impurity signal, and those with obvious fluorescence signal. After preprocessing Raman spectra (1450 $^{-1}$ , 550  $\text{cm}^{-1}$ ) via baseline correction and normalization with max intensity, batch calculations of the  $^{13}\text{C}$  ratio [ $^{13}\text{C}/(^{12}\text{C}+^{13}\text{C})$ ] from at least 50 single-cell Raman spectra were undertaken within each group. The  $^{13}\text{C}$  ratio, reflecting the metabolic activity of a single cell, was calculated by dividing the  $^{13}\text{C}$  band area (1480–1490  $\text{cm}^{-1}$ ) by the sum of the  $^{13}\text{C}$  and  $^{12}\text{C}$  characteristic band areas (1510–1530  $\text{cm}^{-1}$ ). At least three independent repeats were conducted separately for each experiment. For the Raman spectra data, those from one randomly chosen sample from the three independent experiments were presented. All statistical analyses were performed using R (>Version 4.0) by customized scripts. The corresponding figures were plotted via the ggplot 2 package. Figs. 1 and 2A were created with BioRender.com.

## 3. Results and discussions

### 3.1. Overview of the iCyanVS strategy for fast-growing individual screening directly from an artificial mutant library

To screen the fast-growing phenotypes of cyanobacteria from an artificial mutant library, the iCyanVS strategy was proposed which include two steps: the vitality test via single-cell Resonance Raman-SIP,

and the Raman-activated cell sorting coupled to single-cell sequencing via the RAGE-Seq technique (Fig. 1). The vitality test aims to establish the relationship between specific Raman signals and the metabolic and growth activities of cyanobacteria. Specifically, the cyanobacterial mutant library was pretreated for stress exposure under a certain stress condition and then incubated in medium containing  $\text{NaH}^{13}\text{CO}_3$  under the same stress conditions for a duration. The resulted sample which includes cells exhibiting distinct SCRS due to their different metabolic activities in stress response was then analyzed using Raman Microspectroscopy. In a SCRS, the Raman bands for carotenoids are proper biomarkers for the red-shifts that quantify the extent of  $^{13}\text{C}$  incorporation, due to their characteristic Raman signal, their relatively high intracellular contents, and their resonance Raman signals that are much stronger than other metabolites. The carotenoid signal intensity was associated with the incubation time of  $\text{NaH}^{13}\text{CO}_3$  and the metabolic and growth activity of cyanobacteria. Based on the red-shift of Raman bands for carotenoids in a SCRS, the  $^{13}\text{C}$  incorporation ratio [ $^{13}\text{C}/(^{12}\text{C}+^{13}\text{C})$ ] was employed to model the metabolic activity and the growth rate of each individual cyanobacteria cell. To decode the single-cell genotype or complete genome sequence that is associated with the SCRS-modeled phenotype, RAGE-Seq was employed to screen and then sort the single cells with targeted phenotype, due to its advantages in maximally preservation of metabolic vitality [36] and in production of high-coverage one-cell genome sequences [37–40].

Specifically, the individual cells are screened via SCRS in an aquatic, vitality-preserving environment, and then the individual cells with targeted SCRS are precisely packaged in a picoliter microdroplet and readily exported in a precisely indexed, “one-cell-one-tube” manner. Such integration of picoliter microdroplet encapsulation into Raman-activated sorting ensures low-bias amplification and thus high-coverage sequencing of the one-cell genome that is directly linked to

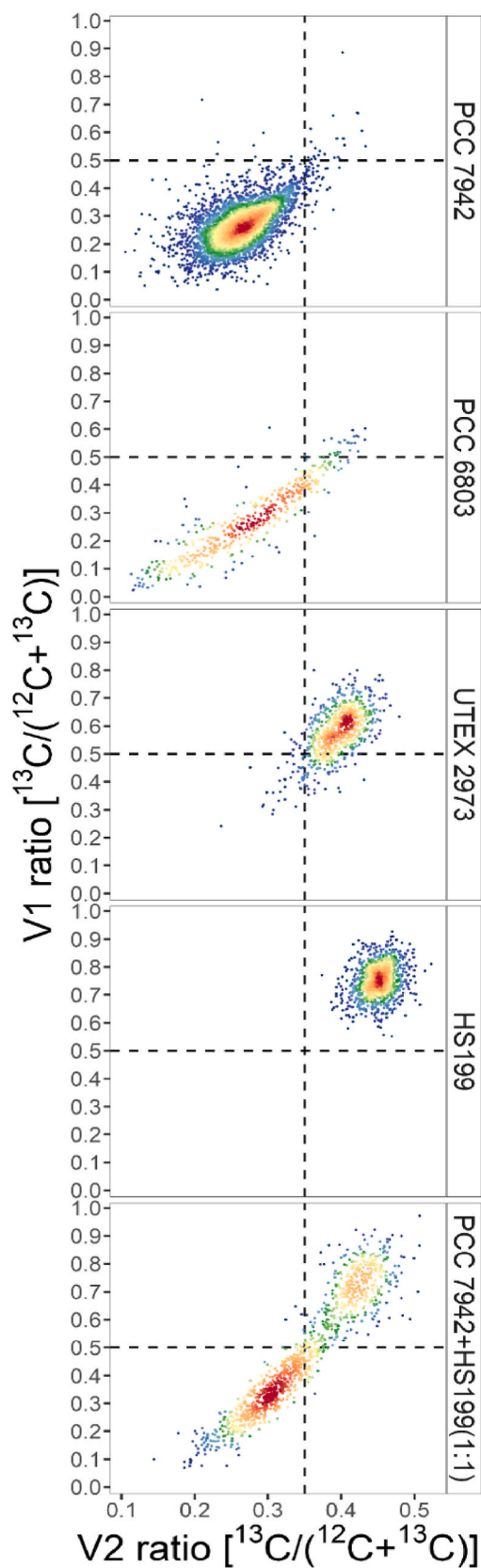


**Fig. 3.** Single-cell metabolic activity of the cyanobacterial strains of PCC 7942, PCC 6803, UTEX 2973, HS199, and PCC 7942 mixed with HS199 (PCC 7942: HS199 = 1: 1) in a mock mutant community. The ratios of v1 and v2 were used to represent the metabolic activity, and the red to blue gradient represents the density from high to low. The dashed line indicates the threshold for distinguishing the metabolic activity of different strains.

the cell's metabolic phenotype (Fig. 1).

### 3.2. Metabolic activity labeling and vitality tests via Raman-SIP

Different cyanobacterial cells exhibit distinct growth rates and metabolic activities under levels of stress [41]. Fed with  $\text{NaH}^{13}\text{CO}_3$  after stress exposure, cells that exhibit higher vitality would carry a strong  $^{13}\text{C}$  incorporation ratio, suggesting their stronger stress tolerance and correspondingly, higher growth rate under stress (Fig. 2A). To establish the relationship between specific Raman signals and the metabolic and growth activity of cyanobacteria, first, the growth curves of PCC 7942 with different concentrations of  $\text{NaHCO}_3$  as the only carbon source were derived. Under  $\text{NaHCO}_3$  concentrations that are greater than 50 mM, the growth of PCC 7942 can be maintained for at least 48 h (Fig. S1), thus 100 mM  $\text{NaHCO}_3$  was chosen as the carbon source in all subsequent experiments. The resonance Raman spectra of carotenoids display characteristic Raman bands (Fig. 2B): v1, v2, and v3. The sharp and strong v1 (stretching mode of the C=C bonds at  $\sim 1515\text{ cm}^{-1}$ ), v2 (stretching mode of the C-C bonds at  $\sim 1155\text{ cm}^{-1}$ ), and v3 (deformation of the methyl groups at  $\sim 1003\text{ cm}^{-1}$ ) peaks can be unambiguously assigned to carotenoids [42]. In addition, the Raman bands of carotenoids displayed a red-shift due to the active  $^{13}\text{C}$  incorporation by cells: the v1, v2, and v3 bands shifted to 1485, 1130, and  $990\text{ cm}^{-1}$  from the original 1520, 1160, and  $1005\text{ cm}^{-1}$  in SCRS of  $^{12}\text{C}$  cells after growth in  $\text{NaH}^{13}\text{CO}_3$ , which was similar to the phenomena reported in previous work with *Synechococcus* sp. PCC 7002 grown in  $\text{NaH}^{13}\text{CO}_3$  [26]. In addition, the signal intensity of  $^{13}\text{C}$  incorporation was closely related to the culture time with  $\text{NaH}^{13}\text{CO}_3$  as the sole carbon source (Fig. 2C), in that the proportion of  $^{13}\text{C}$  incorporation ratio rapidly increased from 2 h and reached a stable labeling state after 36 h (Fig. 2B). Hence, in subsequent experiments, we used the  $^{13}\text{C}$  incorporation ratio in a certain incubation time before reaching a steady state as criteria, so as to identify and sort those cyanobacteria cells that actively take in  $\text{NaH}^{13}\text{CO}_3$ .

### 3.3. Performance of Raman-SIP in evaluating and screening a previously known fast-growing cyanobacteria strain under high-light conditions

To validate the performance of the Raman-SIP system in screening strains with fast-growing characteristics, the cyanobacterial strains PCC 7942, *Synechococcus elongatus* UTEX 2973 (hereafter UTEX 2973), and *Synechocystis* sp. PCC 6803, and a mutant strain HS199 with different growth rates under high light conditions were evaluated. Among them, UTEX 2973 is a recently isolated cyanobacterial strain that has a faster growth rate and better tolerance to high temperature and high light than PCC 7942 and PCC 6803 [43,44]. HS199 is a mutant strain that enhances the high light tolerance of *Synechococcus* by upregulating shikimate kinase expression [41]. All the strains were determined under high light conditions ( $1400\text{ }\mu\text{mol photons m}^{-2}\text{s}^{-1}$ ) with  $\text{NaH}^{13}\text{CO}_3$  as the sole carbon source. The results indicated that the mutant strains HS199 and UTEX 2973 maintained rapid growth under high light culture conditions, and their  $\text{OD}_{730\text{nm}}$  values were increased by 2.7-fold and 1.8-fold compared with PCC 7942 after 12 h of culture under high light conditions (Fig. S2). In addition, the  $\text{OD}_{730\text{nm}}$  of the mixed culture of PCC 7942 and HS199 (initial inoculation amount PCC 7942: HS199 = 1:1) was intermediate between PCC 7942 and HS199.

The SCRS spectral analysis of 1000 single cells from each sample indicated that the metabolic activity of HS199 was significantly higher than that of the other strains (Fig. 3). The metabolic activity of UTEX 2973 was significantly higher than that of PCC 7942 and PCC 6803, which was consistent with the growth phenotype. In addition, there was no significant difference in growth between PCC 6803 and PCC 7942, but the metabolic activity of PCC 7942 was still slightly higher than that of PCC 6803, which is also in agreement with previously reported growth characteristics [45]. Interestingly, the Raman ratio of 1000 single cells were diverse, especially for PCC 7942 and PCC 6803,

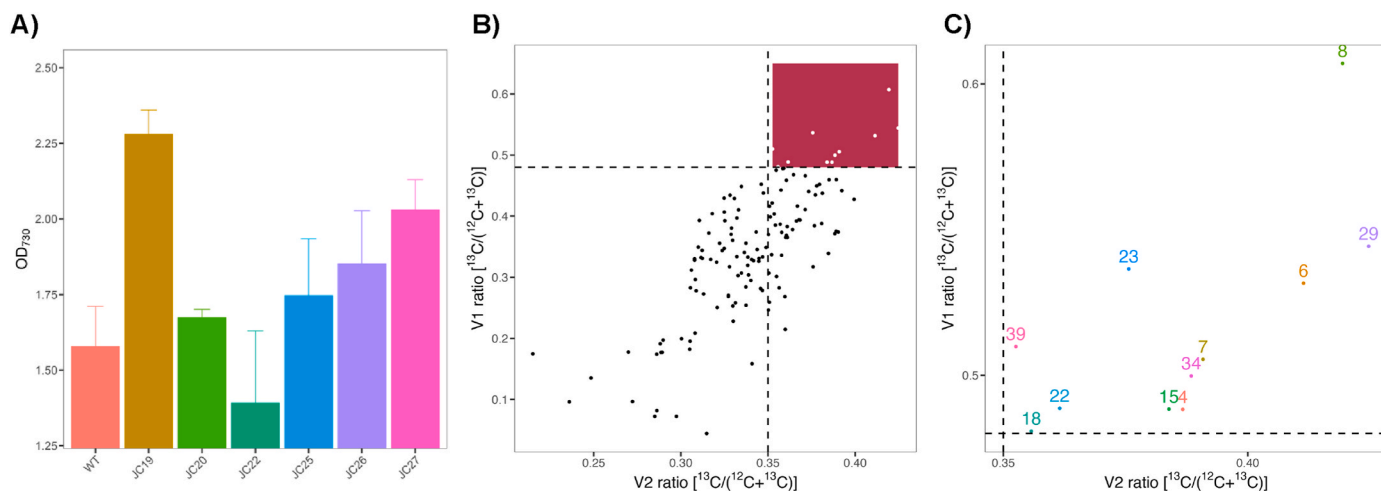


**Fig. 4.** Growth and metabolic activity of the cyanobacterial mutant library. A) The  $OD_{730nm}$  of WT and different mutants (JC19, JC20, JC22, JC25, JC26, JC27) under salt stress conditions; B) The metabolic activity of 130 randomly selected cells. The dashed line indicates the threshold for screening the high vitality cyanobacteria; C) Source-tracking of the selected cells with high metabolic activity.

suggesting that different single cells of the same species had different metabolic activity under high light condition. The reason might be that different single cells responded differently to high-light stress at the transcription and translation levels. Early study also showed that the PCC 6803 had an increasing gene-expression heterogeneity after a certain period of nitrogen-starvation stress [46]. In the near future, it is expected to explore its internal regulatory mechanism through single-cell transcriptome. Moreover, the dispersion degree of the mixed culture of PCC 7942 and HS199 was relatively large, because the metabolic activity of PCC 7942 and HS199 was different under high light conditions. Taken together, the Raman-SIP system can distinguish the growth rate and metabolic activity of different strains by the  $^{13}C$  incorporation ratio of carotenoids, which could be applied to screen fast-growing strains under stress conditions.

### 3.4. Identifying the fastest growing strain by RAGE-Seq from the artificial mutant library

To further screen high vitality cyanobacteria from non-model cyanobacteria strains and different mutants artificially constructed by RAGE-Seq, a Raman-SIP mock mutant library was built. Sigma ( $\sigma$ ) factors are key regulators of global gene expression patterns that dictate the fate of metabolic pathways in cyanobacteria [47]. In recent years, an important strategy based on regulating the levels of  $\sigma$  factors, termed transcription factor engineering, has already been developed and adopted for engineering the complex metabolism and physiological phenotypes of diverse microorganisms [48]. The use of this approach alters the global expression of specific subsets of genes that can result in a positive impact on cell robustness [49]. Meanwhile, large-scale cultivation of cyanobacteria with seawater is necessary for industrial biotechnological applications [8]. Thus, it is urgent to improve the salt tolerance of freshwater PCC 7942 for the future application of this promising chassis for green fuels and chemical production. Therefore, all the  $\sigma$  factors in PCC 7942 were overexpressed, and mutant libraries including PCC 7942 and JC19-JC27 were constructed to screen the fast-growing mutant under salt stress (Table 1). Furthermore, the growth curves of all mutant strains and PCC 7942 (WT) were analyzed under normal and salt stress conditions (Fig. S3). The growth of JC19 was increased by 44 %, which was significantly higher than that of the wild type (Fig. 4).

To screen salt-tolerant strains by RAGE from the mutant library more efficiently, the growth in bulk culture and metabolic activity of PCC 7942 at the single-cell level under different NaCl concentrations were

**Table 2**

Identification of the individual cyanobacterial cells with high metabolic activity.

Number	V1_ratio	V2_ratio	Identification
39	0.509	0.353	JC19
4	0.488	0.387	JC19
29	0.544	0.424	JC19
6	0.532	0.411	JC19
7	0.505	0.391	WT
8	0.607	0.419	JC19
34	0.499	0.388	JC19
15	0.488	0.384	JC19
18	0.480	0.356	<sup>a</sup>
22	0.488	0.362	JC19
23	0.536	0.376	<sup>a</sup>

<sup>a</sup> False-positive: No PCR products were amplified.

tested (Fig. S4). The metabolic activity of PCC 7942 at the single-cell level decreased with increasing salt concentration, which had a positive correlation with the growth phenotype. Herein, the 0.35 M NaCl was chosen to screen the salt-tolerant strains in the following experiments. All mutant strains and WT were mixed in a certain proportion to build a mutant library (1/60 for each mutant, 54/60 for WT). A total of 130 single cells were selected and analyzed by Raman-SIP (Fig. 4B). According to the metabolic activity threshold set of different strains under the high light condition, the individual cells in the top 8 % of metabolic activity were selected for MDA amplification and targeted gene verification (Fig. 4C): 72 % of the single cells were identified as strain JC19 (overexpressing the  $\sigma$  factor *rpoD1*) (Table 2), suggesting an enrichment ratio of JC19 (from the 1.6 % before sorting to the 72 % after sorting). During the process, two situations could lead to false positives: one is the result of PCR amplification with no product, and the other is the result of sequencing showing a wild-type phenotype. In the first case, after single-cell sorting, the experiments involving MDA and PCR had a certain success rate, meaning not all single cells could obtain valid PCR results, such as No. 18 and 23 in Table 2. In the second case, where sequencing results showed a wild-type phenotype, it could be that single-cell phenotypic heterogeneity resulting from transcriptional variations. Wild-type strain with higher single-cell activity might also be sorted due to the fact that the reference threshold is not absolutely accurate. JC19 exhibits higher metabolic activity and a faster growth rate under salt stress. In addition, in the process of preculture and labeling, strain JC19, as the dominant strain, had a certain degree of enrichment, which was consistent with the enhancement of HS199 under high-light stress conditions.

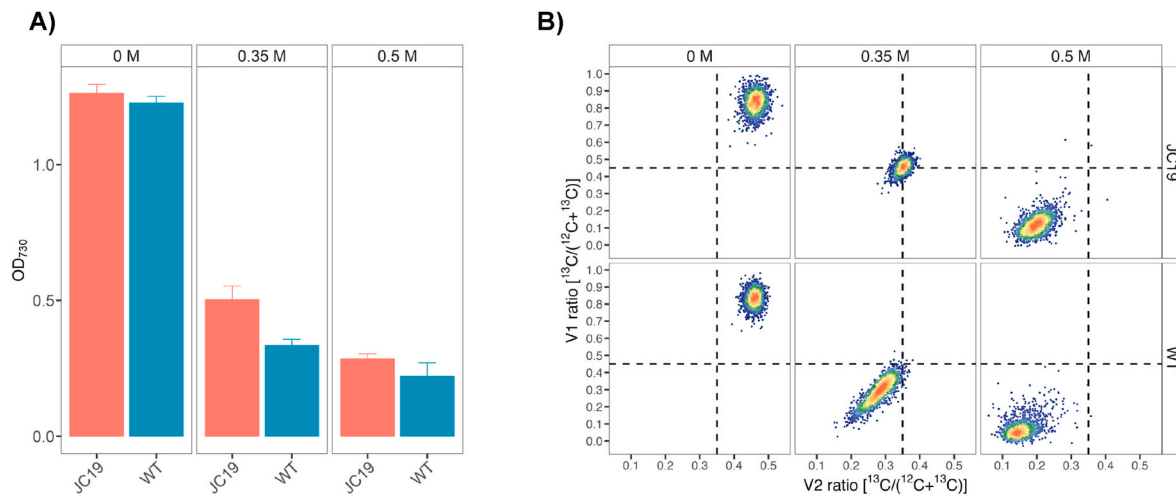


**Fig. 5.** Growth and single-cell metabolic activity analysis of PCC 7942 and mutant strain JC19 under different salt concentrations. A) OD<sub>730nm</sub> for PCC 7942 under 0 M, 0.35 M, and 0.5 M NaCl concentration conditions; B) The metabolic activity of PCC 7942 and JC19 at the single-cell level under different concentrations of NaCl.

Furthermore, the metabolic activities of JC19 and WT at the single-cell level under different salt concentrations were also analyzed. No significant difference between the two strains under normal conditions (Fig. 5). The metabolic activity of JC19 was significantly higher than that of WT at 0.35 M NaCl, and slightly higher at 0.5 M NaCl. In addition, the overall metabolic activity decreased with increasing salt concentration. Thus, strain JC19 grew faster under salt stress. In conclusion, mutant strains with high metabolic activity identified by RAGE at the single-cell level also had obvious growth advantages in the population-level growth phenotype. These findings are of great significance for the screening of fast-growing strains of cyanobacteria and provide references for high-throughput screening of other phenotypes such as growth, resistance, and metabolite synthesis.

#### 4. Conclusions

Traditional culture-based screening paradigm usually requires plotting of the growth curve based on OD, which would take at least 7–10 days and thus is time-consuming, of low throughput, and consuming a large amount of medium. On the other hand, natural chlorophyll autofluorescence can be monitored to track growth rate by the microdroplet platform, however, this is also dependent on the time-consuming cell culture and moreover growth-phenotype sorting of the microdroplet-based cyanobacterial cultures has not been realized [9].

In contrast, iCyanVS, by exploring the rich information content in a SCRS, can quickly screen highly active single-cells (0.1 s/single-cell) after only hours of stable isotope incubation. In addition, ability to probe growth rate-related or carbon fixation-related phenotypes at single-cell resolution is highly valuable for tackling genetically heterogeneous samples such as a mutant library, as this would allow the mutants to be phenotypically screened under their *in situ* conditions, regardless of their relative growth competitiveness among mutant cells in the consortium. Furthermore, as carotenoids are widely found in photosynthetic organisms, this approach is broadly applicable to not just cyanobacteria but to other types of microalgae and higher plants.

In this example, using PCC 7942 and the highlight-tolerant mutant strain HS199 as a model whose growth rates differ in bulk cultures, the iCyanVS system discriminated between cells of the two species after just 12 h of incubation, and then identified the salt-tolerant strain JC19 under salt stress from the mutant library via single-cell RAGE-Seq. The results represent an advance over previous cyanobacteria-phenotyping studies since the phenotyping measurement is directly based on the metabolic activity properties of every single cell. Therefore, the advantages of iCyanVS, including being culture-free, identifying single-cell

metabolic activity, high throughput, and high accuracy, suggest its promising use as a broadly applicable approach for efficiently mining fast-growing autotrophic chassis cells or for dissecting phenotype-genotype links of cyanobacteria at single-cell resolution.

#### CRedit authorship contribution statement

**Jinyu Cui:** Investigation, Writing – original draft. **Rongze Chen:** Investigation, Writing – original draft. **Huili Sun:** Investigation, Writing – original draft. **Yingyi Xue:** Investigation, Writing – original draft. **Zhidian Diao:** Investigation, Writing – original draft. **Jingyun Song:** Investigation, Writing – original draft. **Xiaohang Wang:** Investigation, Writing – original draft. **Jia Zhang:** Investigation, Writing – original draft. **Chen Wang:** Investigation, Writing – original draft. **Bo Ma:** Conceptualization, Supervision, Funding acquisition, Writing – review & editing. **Jian Xu:** Conceptualization, Supervision, Funding acquisition, Writing – review & editing. **Guodong Luan:** Conceptualization, Supervision, Funding acquisition, Writing – review & editing. **Xuefeng Lu:** Conceptualization, Supervision, Funding acquisition, Writing – review & editing.

#### Declaration of competing interest

The authors declare that they have no known competing financial interests or personal relationships that could have appeared to influence the work reported in this paper.

#### Acknowledgements

This work was supported by the National Key Research and Development Program of China (Grant number 2021YFA0909700), the National Natural Science Foundation of China (Grant numbers 32070084, 32270103, 32271484, 32300058), the Youth Innovation Promotion Association CAS (to Guodong Luan), Postdoctoral Innovation Project of Shandong Province (Grant number SDCX-ZG-202202036) and Postdoctoral Science Foundation of China (Grant number 2021M703320), and the Shandong Taishan Scholarship (to Xuefeng Lu, and to Guodong Luan).

#### Appendix A. Supplementary data

Supplementary data to this article can be found online at <https://doi.org/10.1016/j.synbio.2023.11.001>.

## References

- [1] Stanier RY, Cohen-Bazire G. Phototrophic prokaryotes: the cyanobacteria. *Annu Rev Microbiol* 1977;31(1):225–74.
- [2] Zhu H, Li Y. Turning light into electricity, biologically. *Green Carbon* 2023;1:14–9.
- [3] Liu Z, Shi S, Ji Y, Wang K, Tan T, Nielsen J. Opportunities of CO<sub>2</sub>-based biorefineries for production of fuels and chemicals. *Green Carbon* 2023;1(1): 75–84.
- [4] Angermayr SA, Hellingwerf KJ, Lindblad P, de Mattos MJ. Energy biotechnology with cyanobacteria. *Curr Opin Biotechnol* 2009;20(3):257–63.
- [5] Khatoun H, Leong LK, Rahman NA, Mian S, Begum H, Banerjee S, et al. Effects of different light source and media on growth and production of phycobiliprotein from freshwater cyanobacteria. *Bioresour Technol* 2018;249:652–8.
- [6] Xiong W, Cano M, Wang B, Douchi D, Yu J. The plasticity of cyanobacterial carbon metabolism. *Curr Opin Chem Biol* 2017;41:12–9.
- [7] Luan G, Zhang S, Lu X. Engineering cyanobacteria chassis cells toward more efficient photosynthesis. *Curr Opin Biotechnol* 2019;62:1–6.
- [8] Cui J, Sun T, Chen L, Zhang W. Engineering salt tolerance of photosynthetic cyanobacteria for seawater utilization. *Biotechnol Adv* 2020;43:107578.
- [9] Best RJ, Lyczakowski JJ, Abalde-Cela S, Yu Z, Abell C, Smith AG. Label-free analysis and sorting of microalgae and cyanobacteria in microdroplets by intrinsic chlorophyll fluorescence for the identification of fast growing strains. *Anal Chem* 2016;88(21):10445–51.
- [10] Binder S, Schendzielorz G, Stähler N, Krumbach K, Hoffmann K, Bott M, et al. A high-throughput approach to identify genomic variants of bacterial metabolite producers at the single-cell level. *Genome Biol* 2012;13. R40 - R.
- [11] Zeng W, Guo L, Xu S, Chen J, Zhou J. High-throughput screening technology in industrial biotechnology. *Trends Biotechnol* 2020;38(8):888–906.
- [12] Unrean P, Champreda V. High-throughput screening and dual feeding fed-batch strategy for enhanced single-cell oil accumulation in *Yarrowia lipolytica*. *BioEnergy Res* 2017;10.
- [13] Zenobi R. Single-cell metabolomics: analytical and biological perspectives. *Science* 2013;342(6163):1201. --.
- [14] Stepanauskas R. Single cell genomics: an individual look at microbes. *Curr Opin Microbiol* 2012;15(5):613–20.
- [15] He Y, Zhang P, Huang S, Wang T, Ji Y, Xu J. Label-free, simultaneous quantification of starch, protein and triacylglycerol in single microalgal cells. *Biotechnol Biofuels* 2017;10:275.
- [16] Nitta N, Sugimura T, Isozaki A, Mikami H, Hiraki K, Sakuma S, et al. Intelligent image-activated cell sorting. *Cell* 2018;175(1):266–276 e13.
- [17] Li M, Ashok PC, Dholakia K, Huang WE. Raman-activated cell counting for profiling carbon dioxide fixing microorganisms. *J Phys Chem A* 2012;116(25): 6560–3.
- [18] Hammar P, Angermayr SA, Sjöström SL, van der Meer J, Hellingwerf KJ, Hudson EP, et al. Single-cell screening of photosynthetic growth and lactate production by cyanobacteria. *Biotechnol Biofuels* 2015;8:193.
- [19] Abalde-Cela S, Gould A, Liu X, Kazamia E, Smith AG, Abell C. High-throughput detection of ethanol-producing cyanobacteria in a microdroplet platform. *J R Soc Interface* 2015;12(106).
- [20] Li M, Canniffe DP, Jackson PJ, Davison PA, FitzGerald S, Dickman MJ, et al. Rapid resonance Raman microspectroscopy to probe carbon dioxide fixation by single cells in microbial communities. *ISME J* 2012;6(4):875–85.
- [21] Venkata HNN, Shigeto S. Stable isotope-labeled Raman imaging reveals dynamic proteome localization to lipid droplets in single fission yeast cells. *Chem Biol* 2012; 19(11):1373–80.
- [22] Withnall R, Chowdhry BZ, Silver J, Edwards HGM, C de Oliveira LF. Raman spectra of carotenoids in natural products. *Spectrochim Acta A* 2003;59(10):2207–12.
- [23] Xu J, Ma B, Su X, Huang S, Xu X, Zhou X, et al. Emerging trends for microbiome analysis: from single-cell functional imaging to microbiome big data. *Engineering* 2017;3(1):66–70.
- [24] Huang WE, Griffiths RI, Thompson IP, Bailey MJ, Whiteley AS. Raman microscopic analysis of single microbial cells. *Anal Chem* 2004;76(15):4452–8.
- [25] Tao Y, Wang Y, Huang S, Zhu P, Huang WE, Ling J, et al. Metabolic-activity-based assessment of antimicrobial effects by D(2)O-labeled single-cell Raman microspectroscopy. *Anal Chem* 2017;89(7):4108–15.
- [26] Jing X, Gou H, Gong Y, Su X, Xu L, Ji Y, et al. Raman-activated cell sorting and metagenomic sequencing revealing carbon-fixing bacteria in the ocean. *Environ Microbiol* 2018;20(6):2241–55.
- [27] Wang Y, Song Y, Tao Y, Muhamadali H, Goodacre R, Zhou NY, et al. Reverse and multiple stable isotope probing to study bacterial metabolism and interactions at the single cell level. *Anal Chem* 2016;88(19):9443–50.
- [28] Wang Y, Huang WE, Cui L, Wagner M. Single cell stable isotope probing in microbiology using Raman microspectroscopy. *Curr Opin Biotechnol* 2016;41: 34–42.
- [29] Berry D, Mader E, Lee TK, Woebken D, Wang Y, Zhu D, et al. Tracking heavy water (D<sub>2</sub>O) incorporation for identifying and sorting active microbial cells. *Proc Natl Acad Sci USA* 2015;112(2):E194–203.
- [30] Zhu P, Ren L, Zhu Y, Dai J, Liu H, Mao Y, et al. Rapid, automated, and reliable antimicrobial susceptibility test from positive blood culture by CAST-R. *mLife* 2022;1(3):329–40.
- [31] Zhang S, Zheng S, Sun J, Zeng X, Duan Y, Luan G, et al. Rapidly improving high light and high temperature tolerances of cyanobacterial cell factories through the convenient introduction of an AtpA-C252F mutation. *Front Microbiol* 2021;12: 647164.
- [32] He Y, Wang X, Ma B, Xu J. Ramanome technology platform for label-free screening and sorting of microbial cell factories at single-cell resolution. *Biotechnol Adv* 2019;37(6):107388.
- [33] Lou W, Tan X, Song K, Zhang S, Luan G, Li C, et al. A specific single nucleotide polymorphism in the ATP synthase gene significantly improves environmental stress tolerance of *Synechococcus elongatus* PCC 7942. *Appl Environ Microbiol* 2018;84(18).
- [34] Yang K, Li HZ, Zhu X, Su JQ, Ren B, Zhu YG, et al. Rapid antibiotic susceptibility testing of pathogenic bacteria using heavy-water-labeled single-cell Raman spectroscopy in clinical samples. *Anal Chem* 2019;91(9):6296–303.
- [35] Wang C, Chen R, Xu J, Jin L. Single-cell Raman spectroscopy identifies *Escherichia coli* persisters and reveals their enhanced metabolic activities. *Front Microbiol* 2022;13:936726.
- [36] Ni H, Jing X, Xiao X, Zhang N, Wang X, Sui Y, et al. Microbial metabolism and necromass mediated fertilization effect on soil organic carbon after long-term community incubation in different climates. *ISME J* 2021;15(9):2561–73.
- [37] Zhu P, Ren L, Zhu Y, Dai J, Liu H, Mao Y, et al. Rapid, automated, and reliable antimicrobial susceptibility test from positive blood culture by CAST-R. *mLife* 2022;1(3):329–40.
- [38] Liu M, Zhu P, Zhang L, Gong Y, Wang C, Sun L, et al. Single-cell identification, drug susceptibility test, and whole-genome sequencing of *Helicobacter pylori* directly from gastric biopsy by clinical antimicrobial susceptibility test ramanometry. *Clin Chem* 2022;68(8):1064–74.
- [39] Xu T, Gong Y, Su X, Zhu P, Dai J, Xu J, et al. Phenome-genome profiling of single bacterial cell by Raman-activated gravity-driven encapsulation and sequencing. *Small* 2020;16(30):e2001172.
- [40] Zhang J, Ren L, Zhang L, Gong Y, Xu T, Wang X, et al. Single-cell rapid identification, in situ viability and vitality profiling, and genome-based source-tracking for probiotics products. *iMeta* 2023;2(3).
- [41] Sun H, Luan G, Ma Y, Lou W, Chen R, Feng D, et al. Engineered hypermutation adapts cyanobacterial photosynthesis to combined high light and high temperature stress. *Nat Commun* 2023;14(1):1238.
- [42] Robert B. Resonance Raman spectroscopy. *Photosynth Res* 2009;101(2):147–55.
- [43] Mueller TJ, Ungerer JL, Pakrasi HB, Maranas CD. Identifying the metabolic differences of a fast-growth phenotype in *Synechococcus* UTEX 2973. *Sci Rep* 2017; 7:41569.
- [44] Ungerer J, Wendt KE, Hendry JI, Maranas CD, Pakrasi HB. Comparative genomics reveals the molecular determinants of rapid growth of the cyanobacterium *Synechococcus elongatus* UTEX 2973. *Proc Natl Acad Sci U S A* 2018;115(50): E11761-E11770.
- [45] Yu J, Liberton M, Cliften PF, Head RD, Jacobs JM, Smith RD, et al. *Synechococcus elongatus* UTEX 2973, a fast growing cyanobacterial chassis for biosynthesis using light and CO<sub>2</sub>. *Sci Rep* 2015;5:8132.
- [46] Wang J, Chen L, Chen Z, Zhang W. RNA-seq based transcriptomic analysis of single bacterial cells. *Integr Biol* 2015;7(11):1466–76.
- [47] Srivastava A, Varshney RK, Shukla P. Sigma factor modulation for cyanobacterial metabolic engineering. *Trends Microbiol* 2021;29(3):266–77.
- [48] Alper H, Stephanopoulos G. Global transcription machinery engineering: a new approach for improving cellular phenotype. *Metab Eng* 2007;9(3):258–67.
- [49] Srivastava A, Summers ML, Sobotka R. Cyanobacterial sigma factors: current and future applications for biotechnological advances. *Biotechnol Adv* 2020;40: 107517.